Plastic debris in the open ocean

Andrés Cózar[a,1], Fidel Echevarría[a], J. Ignacio González-Gordillo[a], Xabier Irigoien[b,c], Bárbara Úbeda[a], Santiago Hernández-León[d], Álvaro T. Palma[e], Sandra Navarro[f], Juan García-de-Lomas[a], Andrea Ruiz[g], María L. Fernández-de-Puelles[h], and Carlos M. Duarte[i,j,k,l]

[a]Área de Ecología, Facultad de Ciencias del Mar y Ambientales, Universidad de Cádiz, Campus de Excelencia Internacional del Mar, E-11510 Puerto Real, Spain; [b]Red Sea Research Center, King Abdullah University of Science and Technology, Thuwal 23955-6900, Kingdom of Saudi Arabia; [c]AZTI, Arrantza eta Elikaigintzarako Institutu Teknologikoa, 20110 Pasaia, Spain; [d]Instituto de Oceanografía y Cambio Global, Universidad de Las Palmas de Gran Canaria, Campus Universitario de Tafira, 35017 Las Palmas de Gran Canaria, Canary Islands, Spain; [e]Fisioaqua, Las Condes, 6513677 Santiago, Chile; [f]Departamento de Ecología, Universidad de Barcelona, E-08028 Barcelona, Spain; [g]Pakea Bizkaia, 48990 Getxo, Spain; [h]Instituto Español de Oceanografía, Centro Oceanográfico de Baleares, 07015 Palma de Mallorca, Spain; [i]Department of Global Change Research, Instituto Mediterráneo de Estudios Avanzados (Universidad de las Islas Baleares-Consejo Superior de Investigaciones Científicas), 07190 Esporles, Spain; [j]The University of Western Australia Oceans Institute and [k]School of Plant Biology, The University of Western Australia, Crawley, WA 6009, Australia; and [l]Faculty of Marine Sciences, King Abdulaziz University, Jeddah 21589, Kingdom of Saudi Arabia

Edited by David M. Karl, University of Hawaii, Honolulu, HI, and approved June 6, 2014 (received for review August 3, 2013)

There is a rising concern regarding the accumulation of floating plastic debris in the open ocean. However, the magnitude and the fate of this pollution are still open questions. Using data from the Malaspina 2010 circumnavigation, regional surveys, and previously published reports, we show a worldwide distribution of plastic on the surface of the open ocean, mostly accumulating in the convergence zones of each of the five subtropical gyres with comparable density. However, the global load of plastic on the open ocean surface was estimated to be on the order of tens of thousands of tons, far less than expected. Our observations of the size distribution of floating plastic debris point at important size-selective sinks removing millimeter-sized fragments of floating plastic on a large scale. This sink may involve a combination of fast nano-fragmentation of the microplastic into particles of microns or smaller, their transference to the ocean interior by food webs and ballasting processes, and processes yet to be discovered. Resolving the fate of the missing plastic debris is of fundamental importance to determine the nature and significance of the impacts of plastic pollution in the ocean.

The current period of human history has been referred as the Plastic Age (1). The light weight and durability of plastic materials make them suitable for a very wide range of products. However, the intense consumption and rapid disposal of plastic products is leading to a visible accumulation of plastic debris (2). Plastic pollution reaches the most remote areas of the planet, including the surface waters of the open ocean. Indeed, high concentrations of floating plastic debris have been reported in central areas of the North Atlantic (3) and Pacific Oceans (4, 5), but oceanic circulation models suggest possible accumulation regions in all five subtropical ocean gyres (6, 7). The models predict that these large-scale vortices act as conveyor belts, collecting the floating plastic debris released from the continents and accumulating it into central convergence zones.

Plastic pollution found on the ocean surface is dominated by particles smaller than 1 cm in diameter (8), commonly referred to as microplastics. Exposure of plastic objects on the surface waters to solar radiation results in their photodegradation, embrittlement, and fragmentation by wave action (9). However, plastic fragments are considered to be quite stable and highly durable, potentially lasting hundreds to thousands of years (2). Persistent nano-scale particles may be generated during the weathering of plastic debris, although their abundance has not been quantified in ocean waters (9).

As the size of the plastic fragments declines, they can be ingested by a wider range of organisms. Plastic ingestion has been documented from small fish to large mammals (10–12). The most evident effects of plastic ingestion are mechanical [e.g., gastrointestinal obstruction in seabirds (13)], but plastic fragments contain contaminants added during plastic manufacture or acquired from seawater through sorption processes [e.g., hydrophobic chemicals (14, 15)]. Recent studies provide evidence that these contaminants can accumulate in the receiving organisms during digestion (14).

Our awareness of the significance of plastic pollution in the ocean is relatively recent, and basic questions remain unresolved. Indeed, the quantity of plastic floating in the ocean and its final destination are still unknown (16). Historical time series of surface plastic concentration in fixed ocean regions show no significant increasing trend since the 1980s, despite an increase in production and disposal (3, 16, 17). These studies suggest that surface waters are not the final destination for buoyant plastic debris in the ocean. Nano-fragmentation, predation, biofouling, or shore deposition have been proposed as possible mechanisms of removal from the surface (3, 9, 16).

On the basis of samples collected on a circumnavigation cruise (Malaspina 2010 expedition), on five regional cruises, and available data from recent studies (3–5, 17–19), we aim to provide a first-order approximation of the load of plastic debris in surface waters of the open ocean. We also examine the size distribution of floating plastic debris collected along the circumnavigation to provide insight into the nature of possible losses of floating plastic from the open ocean surface.

Significance

High concentrations of floating plastic debris have been reported in remote areas of the ocean, increasing concern about the accumulation of plastic litter on the ocean surface. Since the introduction of plastic materials in the 1950s, the global production of plastic has increased rapidly and will continue in the coming decades. However, the abundance and the distribution of plastic debris in the open ocean are still unknown, despite evidence of affects on organisms ranging from small invertebrates to whales. In this work, we synthetize data collected across the world to provide a global map and a first-order approximation of the magnitude of the plastic pollution in surface waters of the open ocean.

Author contributions: A.C., F.E., J.I.G.-G., X.I., and C.M.D. designed research; A.C., F.E., J.I.G.-G., X.I., B.U., S.H.-L., A.T.P., S.N., J.G.-d.-L., A.R., M.L.F.-d.-P., and C.M.D. performed research; A.C., X.I., B.U., S.N., J.G.-d.-L., and M.L.F.-d.-P. contributed new reagents/analytic tools; A.C., J.I.G.-G., B.U., A.T.P., S.N., and J.G.-d.-L. analyzed data; and A.C., F.E., X.I., and C.M.D. wrote the paper.

The authors declare no conflict of interest.

This article is a PNAS Direct Submission.

Freely available online through the PNAS open access option.

[1]To whom correspondence should be addressed. E-mail: andres.cozar@uca.es.

This article contains supporting information online at www.pnas.org/lookup/suppl/doi:10.1073/pnas.1314705111/-/DCSupplemental.

Results and Discussion

The dataset assembled here included 3,070 total samples collected around the world (*SI Appendix*, Table S1). The frequency of occurrence of plastic debris in the surface samples of the open ocean was considerably high (88%; Fig. 1). Nevertheless, the concentration of plastic ranged broadly, spanning over four orders of magnitude across the open ocean. The distribution pattern agreed with those predicted from ocean surface circulation models (6, 7), confirming the accumulation of plastic debris in the convergence zone of each of the five large subtropical gyres. Using the high and low ranges of spatial concentrations measured within 15 major convergence/divergence zones in the global ocean (Fig. 2), we estimate the amount of plastic in the open-ocean surface between 7,000 and 35,000 tons (Table 1). The plastic concentrations per surface area were comparable across each of the five accumulation zones, although the North Pacific Ocean contributed importantly to the global plastic load (between 33 and 35%), mainly owing to the size of this gyre. The plastic load in the North Pacific Ocean could be related to the high human population on the eastern coast of the Asian continent, the most densely populated coast in the world, with one-third of the global coastal population (20). Indeed, the surface plastic concentrations measured in the Kuroshio Current, the western arm of the North Pacific Gyre, can become exceptionally high, including the highest reported for nonaccumulation regions (21, 22).

Continental plastic litter enters the ocean largely through storm-water runoff, flowing into watercourses or directly discharged into coastal waters. Estimating the plastic input to the ocean is a complex task. In the 1970s, the US National Academy of Sciences estimated that the flux of plastic to the world oceans was 45,000 tons per year (23), equivalent to 0.1% of the global production of plastic (24). Since then, the annual production of plastic has quintupled (265 million tons per year in 2010). Around 50% of the produced plastic is buoyant (24), and 60–64% of the terrestrial load of floating plastic to the sea is estimated to be exported from coastal to open-ocean waters (7). Despite the possible inaccuracies of these numbers, a conservative first-order estimate of the floating plastic released into the open ocean from the 1970s (10^6 tons) is 100-fold larger than our estimate of the current load of plastic stored in the ocean.

Examination of the size distribution of plastic debris on the ocean surface shows a peak in abundance of fragments around 2 mm and a pronounced gap below 1 mm (Fig. 3*A*). Similar patterns are found when the data are analyzed separately by ocean basin (*SI Appendix*, Fig. S6). The predominance of fragments in an intermediate interval (1–5 mm) of the plastic size spectra is also a general feature for the oceanic size distributions reported in the past (5, 8). However, experiments on the fragmentation of plastic materials show that the size distribution of fragments generated by a plastic object conforms to a fractal process, spreading over several orders of magnitude and below the size range in our study (25, 26). Cracking patterns of photodegraded plastics are observed at multiple scales, from centimeters to few microns (9). Therefore, the progressive fragmentation of the plastic objects into more and smaller pieces should lead to a gradual increase of fragments toward small sizes. In steady state, the abundance–size distribution should follow a power law, with a scaling exponent equal to the spatial dimension of the plastic objects (i.e., 3, *SI Appendix*, Fig. S8). Likewise, a stable input and fragmentation of large plastic objects should result in a steady volume–size distribution. A model based on fragmentation, without additional losses, gave an abundance–size distribution similar to that sampled, which showed a power exponent of 2.93 ± 0.08, similar to the expected value, but only for size classes larger than 5 mm. Below 5 mm, the observed size distribution diverged from that expected from the model (Fig. 3 *B* and *C*). Because plastic input is progressively transferred toward small-size classes by fragmentation, this divergence results from the gradual accumulation of plastic losses. An assessment of progressive departures of the observed distribution from a conservative distribution indicates that losses are concentrated around sizes of 2.2 mm (Fig. 3*C*). Hence, the paucity of fragments in the lowest part of the size distribution would be explained by the interruption of the downward transfer of plastic at the millimeter scale, unless there is an abrupt nano-fragmentation of the millimeter-sized particles directly into pieces of

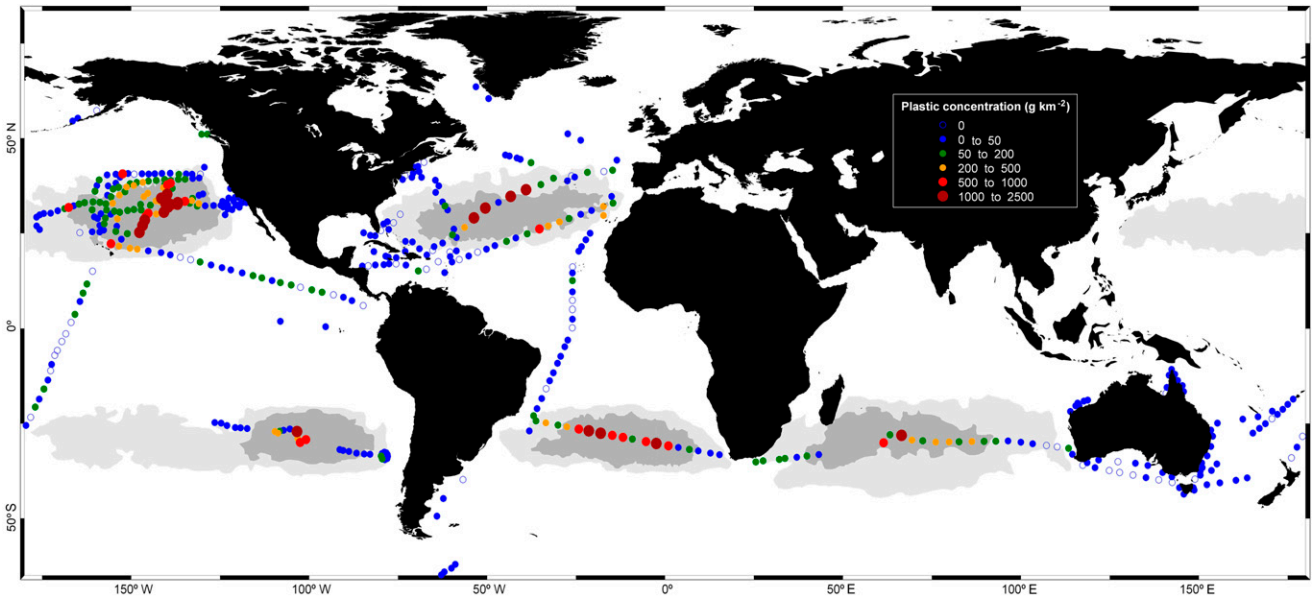

Fig. 1. Concentrations of plastic debris in surface waters of the global ocean. Colored circles indicate mass concentrations (legend on top right). The map shows average concentrations in 442 sites (1,127 surface net tows). Gray areas indicate the accumulation zones predicted by a global surface circulation model (6). Dark and light gray represent inner and outer accumulation zones, respectively; white areas are predicted as nonaccumulation zones. Data sources are described in *SI Appendix*, Table S1. Plastic concentrations along the Malaspina circumnavigation and a latitudinal gradient are graphed in *SI Appendix*, Figs. S4 and S5.

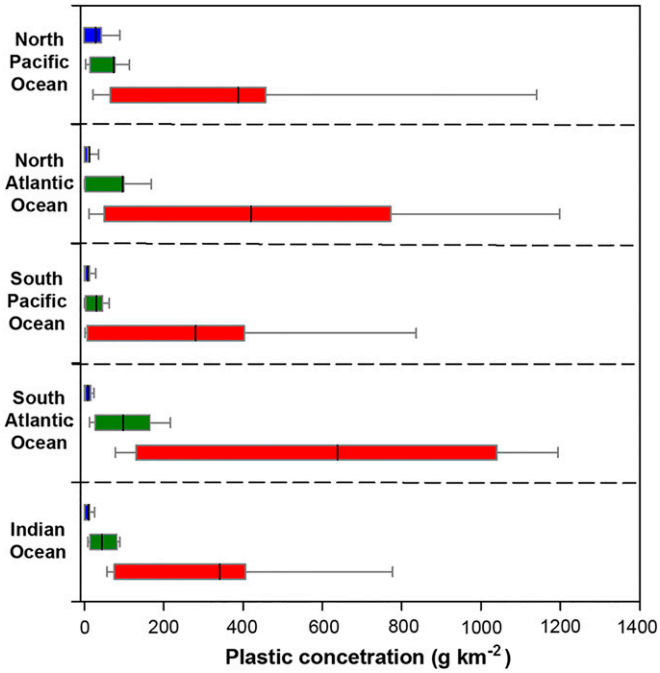

Fig. 2. Ranges of surface plastic concentrations by ocean. Nonaccumulation zone (blue boxes), outer accumulation zone (green boxes), and inner accumulation zone (red boxes). The boundaries of the boxes indicate the 25th and 75th percentiles, the black lines within the box mark the mean, and the whiskers above and below the boxes indicate the 90th and 10th percentiles. Data used in this graph are mapped in Fig. 1. An equivalent analysis for a dataset of plastic concentrations not corrected by wind effects is graphed in *SI Appendix*, Fig. S3.

few microns or smaller, allowing passage through the 200-μm mesh net used (*SI Appendix*, Fig. S9). A sampling bias causing the apparent loss in small sizes can be rejected because the size distribution of nonplastic particles in the same samples followed the characteristic power distribution, with increasing abundances toward smaller sizes (*SI Appendix*, Fig. S12).

Our study reports an important gap in the size distribution of floating plastic debris as well as a global surface load of plastic well below that expected from production and input rates. Together with the lack of observed increasing temporal trends in surface plastic concentration (3, 16, 17), these findings provide strong support to the hypothesis of substantial losses of plastic from the ocean surface. A central question arising from this conclusion is how floating plastic is being removed. Four main possible sinks have been proposed: shore deposition, nanofragmentation, biofouling, and ingestion (3, 9). Although a rigorous attribution of losses to each of these mechanisms is not yet possible, our study provides some insights as to their plausibility. To counterbalance the increase in input rates over the past decades, the removal rate of the presumed sink would also have needed to increase (3). Alternatively, the lack of increasing trends in surface plastic pollution could also be explained from a removal rate much faster than the input into the ocean, with the reduced global load of surface plastic resulting from a delay between input and removal. Another requirement is that the sink must lead to a degradation or permanent sequestration of plastic. Finally, the size distribution of floating plastic debris is evidence for a size-selective loss process or processes.

A selective washing ashore of the millimeter-sized fragments trapped in central areas of the open ocean is unlikely. Likewise, there is no reason to assume that the rate of solar-induced fragmentation increased since the 1980s (3). However, the gap in the plastic size distribution below 1 mm could indicate a fast breaking down of the plastic fragments from millimeter scale to micrometer scale. Recent scanning electron micrographs of the surface of microplastic particles showed indications that oceanic bacterial populations may be contributing to their degradation, potentially intervening in the fragmentation dynamics (27). The scarce knowledge of the biological and physical processes driving the plastic fragmentation leaves room for the possibility of a two-phase fragmentation, with an accelerated breakdown of the photodegraded fragments with dimension of few millimeters.

A preferential submersion of small-sized plastic, with high surface:volume ratio, by ballasting owing to epiphytic growth could also be possible. Once biofouled fragments reach seawater density, they enter the water column as neutrally drifting or slowly sinking particles. Biofouled fragments probably are often incorporated into the sediment in shallow and, particularly, nutrient-rich areas (28), but this may be a less effective mechanism in the deep, open ocean (9, 29). Because the seawater density gradually increase with depth, the slowly sinking plastic, marginally exceeding the surface seawater density, should remain suspended at a depth where its density is equal to that of the medium. Field experiments have shown that biofouled plastic debris undergoes a rapid defouling when submerged, causing the plastic to return to the surface (29). Defouling in deep water could occur, for example, from adverse conditions for the epiphytic organisms (e.g., decreasing irradiance) or the dissolution of carbonates and opal owing to acidic conditions.

The fourth possible sink is ingestion by marine organisms. The size interval accumulating most of plastic losses corresponds to that of zooplankton (mainly copepods and euphausiids). Zooplanktivorous predators represent an abundant trophic guild in the ocean, and it is known that accidental ingestion of plastic occurs during their feeding activity. The reported incidence of plastic in stomachs of epipelagic zooplanktivorous fish ranges from 1 to 29% (30, 31), and in stomachs of small mesopelagic fish from 9 to 35% (10, 32). The most frequent plastic size ingested by fish in all these studies was between 0.5 and 5 mm, matching the predominant size of plastic debris where global losses occur in our assessment. Also, these plastic sizes are commonly found in predators of zooplanktivorous fish (30, 31, 33).

Although diverse zooplanktivorous predators must contribute to the plastic capture at millimeter scale, the small mesopelagic fish likely play a relevant role. They constitute the most abundant and ubiquitous zooplanktivorous assemblage in the open ocean, with densities close to one individual per square meter also in the oligotrophic subtropical gyres (34, 35). Mesopelagic fish live in the middle layer (200–1,000 m deep) of the ocean but migrate to

Table 1. Range of the global load of plastic debris in surface waters of the open ocean

Plastic debris, kilotons	North Pacific Ocean	North Atlantic Ocean	Indian Ocean	South Atlantic Ocean	South Pacific Ocean	Total
Low estimate	2.3	1.0	0.8	1.7	0.8	6.6
Mid estimate	4.8	2.7	2.2	2.6	2.1	14.4
High estimate	12.4	6.7	5.1	5.4	5.6	35.2

Loads by ocean were estimated from the low, mid, and high ranges of plastic concentration measured within major regions in relation to the degree of surface convergence (nonaccumulation zone, outer accumulation zone, and inner accumulation zone). The ranges of plastic concentration by zones are shown in Fig. 2.

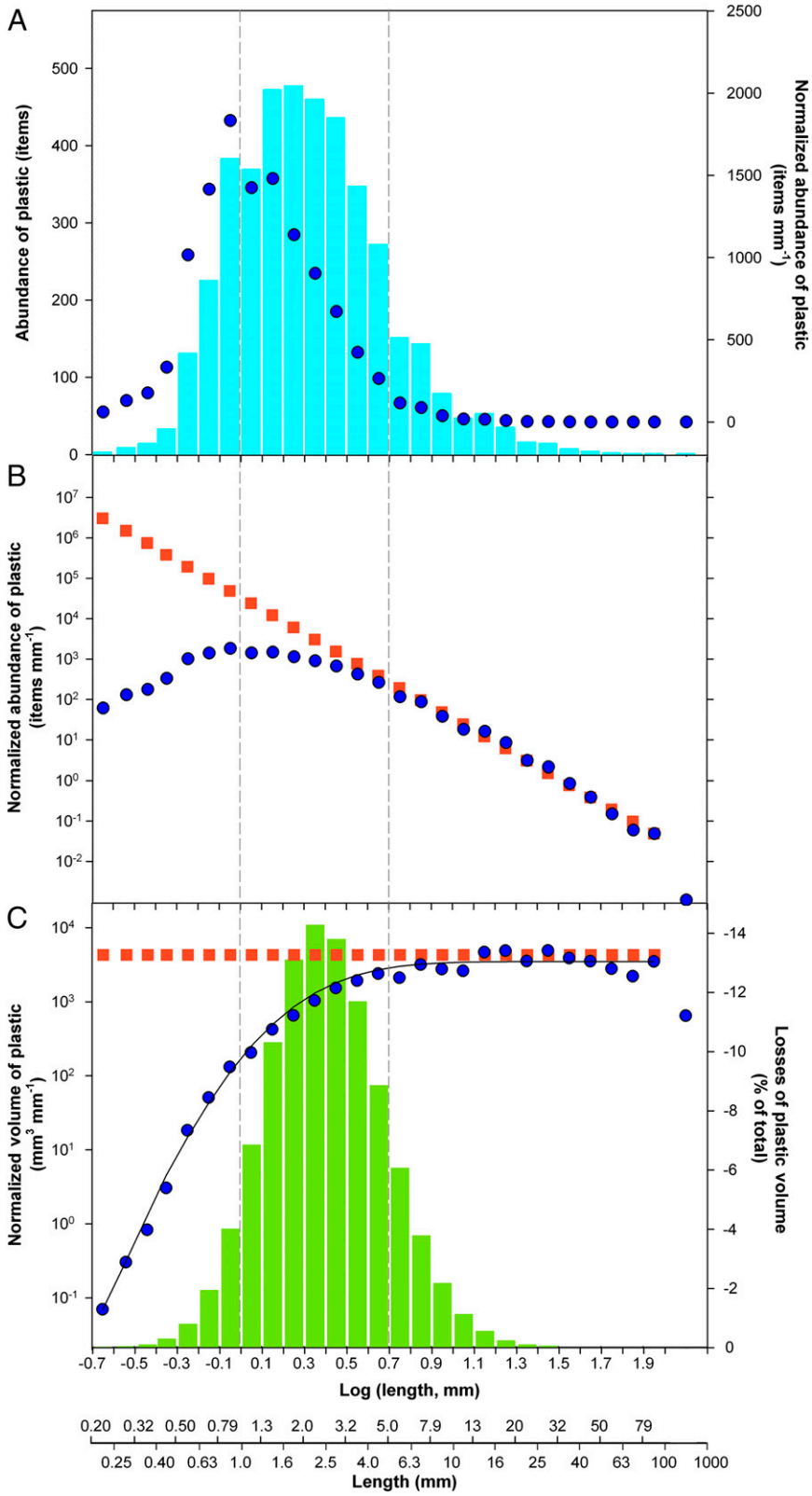

Fig. 3. Size distribution of floating plastic debris collected during the Malaspina circumnavigation at calm conditions. (*A*) Size distribution in abundance (light blue bars) and abundance normalized by the width (in millimeters) of the size class (blue circles). (*B*) Measured (blue circles) and modeled (red squares) size distributions of normalized abundance in logarithmic scale. Modeled distribution was strictly based on fragmentation of large plastic items. (*C*) Measured (blue circles) and modeled (red squares) size distributions in normalized volume. Green bars indicate the estimated losses of plastic volume by size class (Δ_i). After smoothing the measured distribution with a Weibull function (black line, $R = 0.9979$, $P < 0.0001$), losses by size were estimated from its progressive departure from the modeled distribution. Dashed vertical lines through all three graphs correspond to 1-mm and 5-mm size limits. Because plastic presence declined for sizes over 10 cm, modeling analysis was applied up to 10 cm. Note that the largest size class extends from 10 cm to 1 m, the length of the net mouth. Measured size distributions are built from the plastic collected in tows with $u_* < 0.5$ cm·s^{-1} (4,184 plastic items) to avoid wind-mixing effect. An analysis of the effect of wind mixing on plastic size distribution is shown in *SI Appendix*, Fig. S7, and size distributions for the whole Malaspina dataset (7,359 plastic items) are graphed in *SI Appendix*, Fig. S10.

feed in the surface layer at night. Using the plastic content in stomachs, the reported estimates of standing load of plastic in mesopelagic fish (32) are on the same order of magnitude as our estimates of free plastic on the surface. The turnover time of the plastic contained in mesopelagic fish must vary from 1 y to a single day, depending on whether ingested fragments remain in the fish throughout their complete lifespan or are defecated (32). The plastic fragments ingested by small fish can be transferred to larger predators (31, 33), sink with the bodies of dead fish, or be defecated. Gut content of mesopelagic fish is evacuated as long

viscous feces that assume spheroid shapes while sinking at high velocities (around 1,000 $m \cdot d^{-1}$) (36). Hence, microplastic fragments could also reach the bottom via defecation, a proposition that requires further quantitative testing.

Surface losses of large plastic objects by sinking are unaccounted for in our fragmentation model (Fig. 3). However, these large objects, included those in the uppermost part of our plastic size spectrum, are commonly observed on the seafloor (37) and likely contribute significantly to reduce the global load at the surface. Large plastic objects undergo particular biofouling because they can host a wide size range of organisms and often show large cavities (e.g., bags, bottles) that facilitate their ballasting and subsequent sinking.

In the present study, we confirm the gathering of floating plastic debris, mainly microplastics, in all subtropical gyres. The current plastic load in surface waters of the open ocean was estimated in the order of tens of thousands of tons (10,000–40,000). This estimate could be greatly improved through joining sampling efforts particularly in semiclosed seas (e.g., Mediterranean) and the southern hemisphere, where existing data are scarce. Nevertheless, even our high estimate of plastic load, based on the 90th percentile of the regional concentrations, is considerably lower than expected, by orders of magnitude. Our observations also show that large loads of plastic fragments with sizes from microns to some millimeters are unaccounted for in the surface loads. The pathway and ultimate fate of the missing plastic are as yet unknown. We cannot rule out either of the proposed sink processes or the operation of sink processes yet to be identified. Indeed, the losses inferred from our assessment likely involve a combination of multiple sinks. Missing microplastic may derive from nano-fragmentation processes, rendering the very small pieces undetectable to convectional sampling nets, and/or may be transferred to the ocean interior. The abundance of nano-scale plastic particles has still not been quantified in the ocean (9), and the measurements of microplastic in deep ocean are very scarce, although available observations point to a significant abundance of microplastic particles in deep sediments (38), which invokes a mechanism for the vertical transport of plastic particles, such as biofouling or ingestion. Because plastic inputs into the ocean will probably continue, and even increase, resolving the ultimate pathways and fate of these debris is a matter of urgency.

Materials and Methods

From December 2010 to July 2011 the Spanish circumnavigation expedition Malaspina 2010 sampled surface plastic pollution at 141 sites across the oceans. Floating plastic was collected with a neuston net (1.0- × 0.5-m mouth, 200-μm mesh) towed at 2–3 knots for periods 10–15 min (total tows 225). Tow areas were calculated from the readings of a flowmeter in the mouth of the net. Wind speed and water surface density were measured during each tow to estimate average friction velocity in water (u_*) (39).

The material collected by the net was mixed with 0.2-mm-filtered seawater. Subsequently, floating plastic debris was carefully picked out from the water surface with the aid of a dissecting microscope. This examination was repeated at least twice to ensure the detection of all of the smallest plastic particles. To confirm the plastic nature of the material collected in the examinations, Raman spectroscopy was applied to a random subset of particles ($n = 67$). The analysis confirmed the identity of all plastic particles, and polyethylene was found to be the most common polymer type. The vast majority of the plastic items consisted of fragments of larger objects, and industrial resin pellets represented only a small fraction (<2%) of all encountered items. Textile fibers were found only occasionally and were excluded from the analysis because they could be airborne contamination from clothing during the sampling or processing (31).

Plastics extracted from the seawater samples were washed with deionized water and dried at room temperature. The total dry weight of the plastics collected in each tow was recorded. The maximum linear length (l) of the plastic items was measured by high-resolution scanning (*SI Appendix*, Fig. S11) and the image processing Zooimage software (www.sciviews.org). Alternatively, excessively large plastic objects were measured with a ruler. Overall, 7,359 plastic items were measured and separated in 28 size classes to build a size distribution. Size limits of the bins followed a 0.1-log series of l. The width of the uppermost bin extended from 10 cm to the length of the net mouth (100 cm) to account for all sizes that could be collected by the net. The trapping efficiency of fine particles by the mesh was tested from the analysis of the size distribution of nonplastic particles in six tows evenly distributed along the circumnavigation (*SI Appendix*, Fig. S12). Once the plastic particles were picked out from the samples, the size distribution of nonplastic particles was measured by the same methods.

Wind stress can extend the vertical distribution of floating plastic debris into the surface mixing layer, resulting in underestimation of the plastic concentrations measured by the surface tows (0.25 m deep). Thus, the integrated plastic abundance from the surface to the base of the wind-mixed layer (generally <25 m) was estimated with a model dependent on u_* and the numerical concentrations measured in the surface tows (39). Wind-corrected abundances were converted to mass concentrations using a correlation based on simultaneous measurements of total mass and abundance of plastic in 570 worldwide tows (*SI Appendix*, Fig. S13).

Size-Distribution Analysis. A theoretical size distribution of plastic derived from fragmentation was modeled by assuming steady state (large-objects input = small-fragments output, below 0.2 mm). Given that the plastic abundance in a given size class depends on the fragmentation of larger plastic objects already present, we selected a size class with relatively large plastic (reference bin) and projected the plastic amount measured in this bin toward smaller and larger size classes (onward and backward in time). Therefore, the normalized abundance (divided by the width of the size-class interval) of the size class i derived from steady fragmentation was modeled as

$$A_i^f = \frac{A_{ref} \cdot \alpha \cdot l_{ref}^3}{\alpha \cdot l_i^3} = \frac{A_{ref} \cdot l_{ref}^3}{l_i^3}.$$

We used a standard shape for the plastic fragments having the three principal axes proportional to l. Thus, $\alpha \cdot l_i^3$ accounts for the mean volume of the fragments of i, with α being a shape factor and l_i the nominal length for the class i, set at the bin midpoint. A_{ref} is the normalized abundance measured in the reference bin ($i = ref$). The 20- to 25-mm class was selected as reference, although similar results were obtained by selecting other large-size classes.

The normalized volume in each size class derived from fragmentation was modeled as $V_i^f = A_i^f \cdot \alpha \cdot l_i^3 = A_{ref} \cdot \alpha \cdot l_{ref}^3$, being $\alpha = 0.1$, a value corresponding to flat-shaped volume. Because the steady fragmentation of the large-plastic input results in an even volume–size distribution, deviations of the observed size distribution from a conservative distribution can be related to changes in the fragmentation dynamics, inputs of small plastics, or losses (*SI Appendix*, Fig. S9). Estimating volumes from observed abundances ($V_i^* = A_i^* \cdot \alpha \cdot l_i^3$), and after smoothing the resulting volume–size distribution to remove small irregularities, the deviations from a conservative distribution (Δ_i, expressed as percentage of total) were calculated as

$$\Delta_i = \frac{V_{i-1}^* - V_i^*}{\sum_{i=1}^n \left| V_{i-1}^* - V_i^* \right|} = \frac{\left(A_{i-1}^* \cdot l_{i-1}^3\right) - \left(A_i^* \cdot l_i^3\right)}{\sum_{i=1}^n \left| \left(A_{i-1} \cdot l_{i-1}^3\right) - \left(A_i \cdot l_i^3\right) \right|},$$

where $i = 1, 2, \ldots, n$, with n being the lowest size class (0.2–0.25 mm). The denominator accounts for the total deviations accumulated across the entire size range studied. Negative values of Δ_i are related to net plastic losses and positive values to plastic accumulations. Note that Δ_i is independent of the standard plastic shape (α value) used in the computations. Possible variations of α with size were unable to induce changes in the volume–size distribution enough to explain the gap found in small sizes, owing to the extreme scarceness of plastic below 1 mm and the geometrical constrain for α, getting the maximum at 0.52 (spherical shape). Observed plastic abundance in the lowest part of the size spectrum was four orders of magnitude lower than expected from fragmentation (Fig. 3).

The size-distribution analysis is a useful tool to constrain the possible dynamics of marine plastic pollution. Nevertheless, the mechanisms leading to the observed plastic size distributions still are not entirely understood and deserve further attention, resolving the size dependence of the sink/sources processes, as well as testing the framework proposed here (*SI Appendix*, Fig. S9) to identify additional processes.

Spatial Analysis. To analyze the global distribution of floating plastic, data from the Malaspina circumnavigation were combined with additional regional surveys and recent (from 2006 to date) measurements reported by other researchers after data standardization (*SI Appendix*, Table S1).

Concentrations of plastic per surface-water volume were converted to concentrations per surface area from the tow depth, determined according to net type and mouth dimensions (one-half mouth height for neuston nets, three-fourths mouth height for manta nets). Plastic concentrations measured with mesh sizes larger than 0.2 mm were multiplied by a correction factor derived from the plastic size distribution measured in the Malaspina circumnavigation. For 0.3-, 0.5-, and 1.0-mm mesh sizes, numerical underestimation was estimated at 0.4, 2.7, and 21.3%, and mass underestimation at 0.0, 0.4, and 5.0%, respectively. Data reported in numerical concentrations were converted to mass concentrations by using the global relationship found between total mass and abundance (*SI Appendix*, Fig. S13). For data reported without wind correction (3–5, 18), we use satellite winds from the CCMP database (http://podaac.jpl.nasa.gov) to discard samples collected with winds speeds larger than 5 $m \cdot s^{-1}$ ($u_* \sim 0.6$ $cm \cdot s^{-1}$), the threshold above which the effects of wind stress can be significant (39).

The range of the global plastic load in the surface ocean was estimated from the concentration ranges measured over 15 major zones in relation to the degree of surface convergence and by using two different sets of measurements, a wind-corrected dataset and a noncorrected dataset. Using a global circulation model (6), nonaccumulation, outer accumulation, and inner accumulation zones were delimited in each ocean basin to reduce the inaccuracies derived from an uneven distribution of measurements. In addition, plastic measurements were spatially averaged over grid cells of 2° in both latitude and longitude to avoid overweight of areas with high sampling frequency. Overall, 442 grid cells (1,127 net tows) were included in the wind-corrected dataset (Fig. 1 and *SI Appendix*, Table S1). Midrange regional concentrations were calculated from the averaging of the wind-corrected plastic concentrations within each major zone. High-range regional concentrations were calculated from the 90th percentile. We used a wide confidence interval for the plastic load estimate to address variability and possible inaccuracies in the spatial concentrations of plastic. Low-range concentrations were calculated from the averaging of the direct measurements of surface concentrations, without wind correction or discards by high wind mixing (noncorrected dataset: 851 grid cells, 3,070 net tows; *SI Appendix*, Figs. S2 and S3). Global plastic loads in the open-ocean surface were estimated from high, mid, and low regional concentrations and surface areas.

ACKNOWLEDGMENTS. We thank Pakea Bizkaia and the Chilean Navy, which contributed to the sample collection, and K. L. Law, M. C. Goldstein, M. J. Doyle, M. Eriksen, J. Reisser, and their collaborators for their available data. We also thank S. Loiselle and J. Ruiz for his useful suggestions in writing the paper. This research was funded by the Spanish Ministry of Economy and Competitiveness through the Malaspina 2010 expedition project (Consolider-Ingenio 2010, CSD2008-00077) and the Migrants and Active Flux in the Atlantic Ocean project (CTM2012-39587-C04-01). Original data reported in this paper are freely available at http://metamalaspina.imedea.uib-csic.es/geonetwork. This is Campus de Excelencia Internacional del Mar (CEIMAR) Publication 58.

1. Yarsley VE, Couzens EG (1945) *Plastics* (Penguin, London).
2. Barnes DKA, Galgani F, Thompson RC, Barlaz M (2009) Accumulation and fragmentation of plastic debris in global environments. *Philos Trans R Soc Lond B Biol Sci* 364(1526):1985–1998.
3. Law KL, et al. (2010) Plastic accumulation in the North Atlantic subtropical gyre. *Science* 329(5996):1185–1188.
4. Goldstein MC, Rosenberg M, Cheng L (2012) Increased oceanic microplastic debris enhances oviposition in an endemic pelagic insect. *Biol Lett* 8(5):817–820.
5. Eriksen M, et al. (2013) Plastic pollution in the South Pacific subtropical gyre. *Mar Pollut Bull* 68(1–2):71–76.
6. Maximenko N, Hafner J, Niiler P (2012) Pathways of marine debris derived from trajectories of Lagrangian drifters. *Mar Pollut Bull* 65(1–3):51–62.
7. Lebreton LCM, Greer SD, Borrero JC (2012) Numerical modelling of floating debris in the world's oceans. *Mar Pollut Bull* 64(3):653–661.
8. Hidalgo-Ruz V, Gutow L, Thompson RC, Thiel M (2012) Microplastics in the marine environment: A review of the methods used for identification and quantification. *Environ Sci Technol* 46(6):3060–3075.
9. Andrady AL (2011) Microplastics in the marine environment. *Mar Pollut Bull* 62(8): 1596–1605.
10. Boerger CM, Lattin GL, Moore SL, Moore CJ (2010) Plastic ingestion by planktivorous fishes in the North Pacific Central Gyre. *Mar Pollut Bull* 60(12):2275–2278.
11. Choy CA, Drazen JC (2013) Plastic for dinner? Observations of frequent debris ingestion by pelagic predatory fishes from the central North Pacific. *Mar Ecol Prog Ser* 485:155–163.
12. de Stephanis R, Giménez J, Carpinelli E, Gutierrez-Exposito C, Cañadas A (2013) As main meal for sperm whales: Plastics debris. *Mar Pollut Bull* 69(1–2):206–214.
13. Azzarello MY, Van-Vleet ES (1987) Marine birds and plastic pollution. *Mar Ecol Prog Ser* 37:295–303.
14. Teuten EL, et al. (2009) Transport and release of chemicals from plastics to the environment and to wildlife. *Philos Trans R Soc Lond B Biol Sci* 364(1526):2027–2045.
15. Hirai H, et al. (2011) Organic micropollutants in marine plastics debris from the open ocean and remote and urban beaches. *Mar Pollut Bull* 62(8):1683–1692.
16. Thompson RC, et al. (2004) Lost at sea: Where is all the plastic? *Science* 304(5672):838.
17. Law KL, et al. (2014) Distribution of surface plastic debris in the eastern pacific ocean from an 11-year data set. *Environ Sci Technol* 48(9):4732–4738.
18. Doyle MJ, Watson W, Bowlin NM, Sheavly SB (2011) Plastic particles in coastal pelagic ecosystems of the Northeast Pacific ocean. *Mar Environ Res* 71(1):41–52.
19. Reisser J, et al. (2013) Marine plastic pollution in waters around Australia: Characteristics, concentrations, and pathways. *PLoS ONE* 8(11):e80466.
20. Center for International Earth Science Information Network (2012) *National Aggregates of Geospatial Data: Population, Landscape and Climate Estimates Version 3* (National Aeronautics and Space Administration Socioeconomic Data and Applications Center, Palisades, NY). Available at http://sedac.ciesin.columbia.edu/data/set/nagdc-population-landscape-climate-estimates-v3. Accessed October 16, 2012.
21. Day RH, Shaw DG, Ignell SE (1990) The quantitative distribution and characteristics of neuston plastic in the North Pacific Ocean, 1985–88. *Proceedings of the 2nd International Conference on Marine Debris*, eds Shomura RS, Godfrey ML (National Oceanic and Atmospheric Administration, Honolulu), pp 247–266.
22. Yamashita R, Tanimura A (2007) Floating plastic in the Kuroshio Current area, western North Pacific Ocean. *Mar Pollut Bull* 54(4):485–488.
23. National Academy of Sciences (1975) *Assessing Potential Ocean Pollutants: A Report of the Study Panel on Assessing Potential Ocean Pollutants to the Ocean Affairs Board* (National Research Council, Washington, DC).
24. Association of Plastic Manufacturers (2011) *Plastics – the Facts 2011: An analysis of European Plastic Production, Demand and Recovery for 2010* (Plastic Europe, Brussels).
25. Timár G, Blömer J, Kun F, Herrmann HJ (2010) New universality class for the fragmentation of plastic materials. *Phys Rev Lett* 104(9):095502.
26. Kishimura H, Noguchi D, Preechasupanya W, Matsumoto H (2013) Impact fragmentation of polyurethane and polypropylene cylinder. *Physica A* 392(22):5574–5580.
27. Zettler ER, Mincer TJ, Amaral-Zettler LA (2013) Life in the "plastisphere": Microbial communities on plastic marine debris. *Environ Sci Technol* 47(13):7137–7146.
28. Vianello A, et al. (2013) Microplastic particles in sediments of Lagoon of Venice, Italy: First observations on occurrence, spatial patterns and identification. *Estuar Coast Shelf Sci* 130:54–61.
29. Andrady AL, Song Y (1991) Fouling of floating plastic debris under Biscayne Bay exposure conditions. *Mar Pollut Bull* 22(12):117–122.
30. Lusher AL, McHugh M, Thompson RC (2013) Occurrence of microplastics in the gastrointestinal tract of pelagic and demersal fish from the English Channel. *Mar Pollut Bull* 67(1–2):94–99.
31. Foekema EM, et al. (2013) Plastic in north sea fish. *Environ Sci Technol* 47(15): 8818–8824.
32. Davison P, Asch RG (2011) Plastic ingestion by mesopelagic fishes in the North Pacific Subtropical Gyre. *Mar Ecol Prog Ser* 432:173–180.
33. Eriksson C, Burton H (2003) Origins and biological accumulation of small plastic particles in fur seals from Macquarie Island. *Ambio* 32(6):380–384.
34. Lam V, Pauly D (2005) Mapping the global biomass of mesopelagic fishes. *Sea Around Us Proj Newsl* 30:4.
35. Irigoien X, et al. (2014) Large mesopelagic fishes biomass and trophic efficiency in the open ocean. *Nat Commun* 5:3271.
36. Robison BH, Bailey TG (1981) Sinking rates and dissolution of midwater fish fecal matter. *Mar Biol* 65:135–142.
37. Pham CK, et al. (2014) Marine litter distribution and density in European seas, from the shelves to deep basins. *PLoS ONE* 9(4):e95839.
38. Van Cauwenberghe L, Vanreusel A, Mees J, Janssen CR (2013) Microplastic pollution in deep-sea sediments. *Environ Pollut* 182:495–499.
39. Kukulka T, Proskurowski G, Morét-Ferguson S, Meyer DW, Law KL (2012) The effect of wind mixing on the vertical distribution of buoyant plastic debris. *Geophys Res Lett* 39(7):L07601.

SI Appendix for "Plastic debris in the open ocean"

Authors: Andrés Cózar, Fidel Echevarría, Juan I. González-Gordillo, Xabier Irigoien, Bárbara Úbeda, Santiago Hernández-León, Álvaro T. Palma, Sandra Navarro, Juan García-de-Lomas, Andrea Ruiz, María L. Fernández-de-Puelles, Carlos M. Duarte.

Files in this SI Appendix:
Tables S1 to S2
Figures S1 to S13
References S1 to S17

Table S1. Sampling details by source. "Wind-corrected grid cells" indicates the number of 2º x 2º averaged data included in the wind-corrected dataset. "Non-corrected grid cells" indicates the number of 2º x 2º averaged data used for the low estimate of surface plastic pollution. This dataset included data reported by other authors and classified as affected by high wind conditions. Spatial distribution of data by source is shown in Fig. S1. The number of tows by ocean is shown in Table S2.

Region	Wind-corrected grid cells	Non-corrected grid cells	Period	Original unit	Mesh size	Source (vessel)
Malaspina Circumnavigation	141	141	December 2010 to July 2011	g km^{-2}	200 μm	this study (RV Hesperides)
northeastern North Atlantic	12	12	June 2011 to September 2011	g km^{-2}	200 μm	this study (RV Pakea)
southeastern South Atlantic	9	9	December 2012 to February 2013	g km^{-2}	200 μm	this study (RV Pakea)
eastern South Pacific	3	3	March 2009 to November 2011	g km^{-2}	200 μm	this study (RV Poli)
central South Pacific	6	6	March 2012	g km^{-2}	200 μm	this study (RV Aquiles)
west-to-east transect across the North Atlantic	14	14	March 2011	g km^{-2}	1000 μm	this study (RV Sarmiento)
eastern North Atlantic	48	112	February 2006 to December 2008	items km^{-2}	335 μm	ref. (S1)
California Current System (eastern North Pacific)	14	14	April 2006 to January 2007	mg m^{-3}	505 μm	ref. (S2)
Bering Sea (northeastern North Pacific)	3	8	May 2006 to September 2006	mg $m^{-3)}$	505 μm	ref. (S2)
off Vancouver Island (northeastern North Pacific)	2	6	April 2006	mg m^{-3}	505 μm	ref. (S2)
Tropical Pacific	2	9	August 2006 to October 2006	mg m^{-3}	505 μm	ref. (S3)
eastern North Pacific	24	42	August 2009 to October 2010	mg m^{-3}	333 μm	ref. (S3)
east-to-west transect across central South Pacific	15	26	March 2011 to April 2011	g km^{-2}	333 μm	ref. (S4)
waters around Australia	51	51	June 2011 to August 2012	items km^{-2}	333 μm	ref. (S5)
eastern Pacific Ocean	98	398	February 2006 to December 2012	Items km^{-2}	333 μm	ref. (S6)

Table S2. Number of sampled grid cells and surface net tows by oceans for the two datasets used in the spatial analysis of plastic pollution.

	Wind-corrected dataset		**Non-corrected dataset**	
	Grid cells	**Net tows**	**Grid cells**	**Net tows**
North Atlantic Ocean	106	233	170	658
North Pacific Ocean	175	548	440	1682
South Atlantic Ocean	37	54	37	54
South Pacific Ocean	72	165	152	549
Indian Ocean	52	127	52	127
Global Ocean	442	1127	851	3070

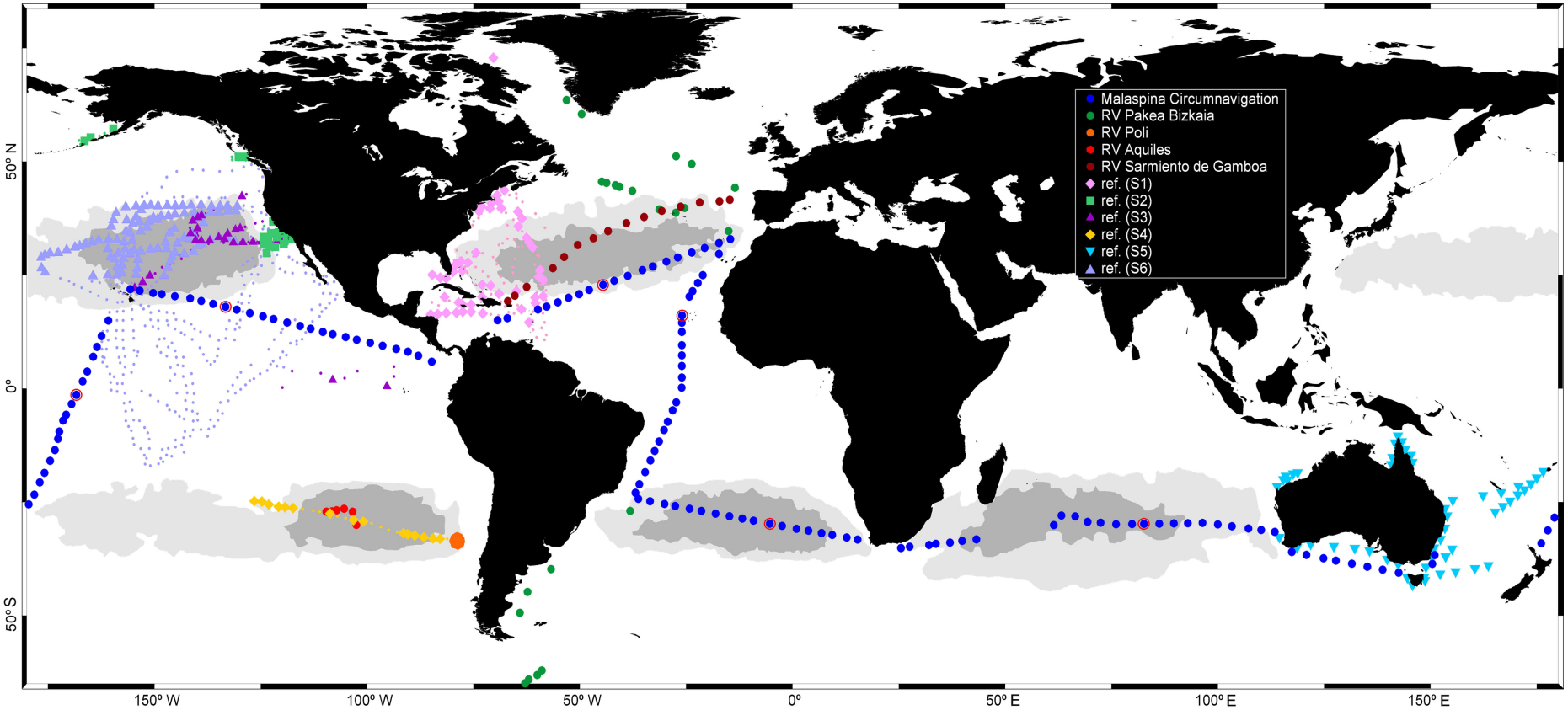

Fig. S1. Spatial distribution of data by sources. Figure legend indicates the vessel for the original data and the bibliographic reference for the datasets published. Large solid symbols show wind-corrected data (442 grid cells, 1127 surface net tows). Small dots show literature data classified as affected by high wind conditions and not included in the wind-corrected dataset (409 grid cells, 1943 surface net tows). Sampling sites where size distribution of non-plastic particles was measured are marked with red circles (see Fig. S12).

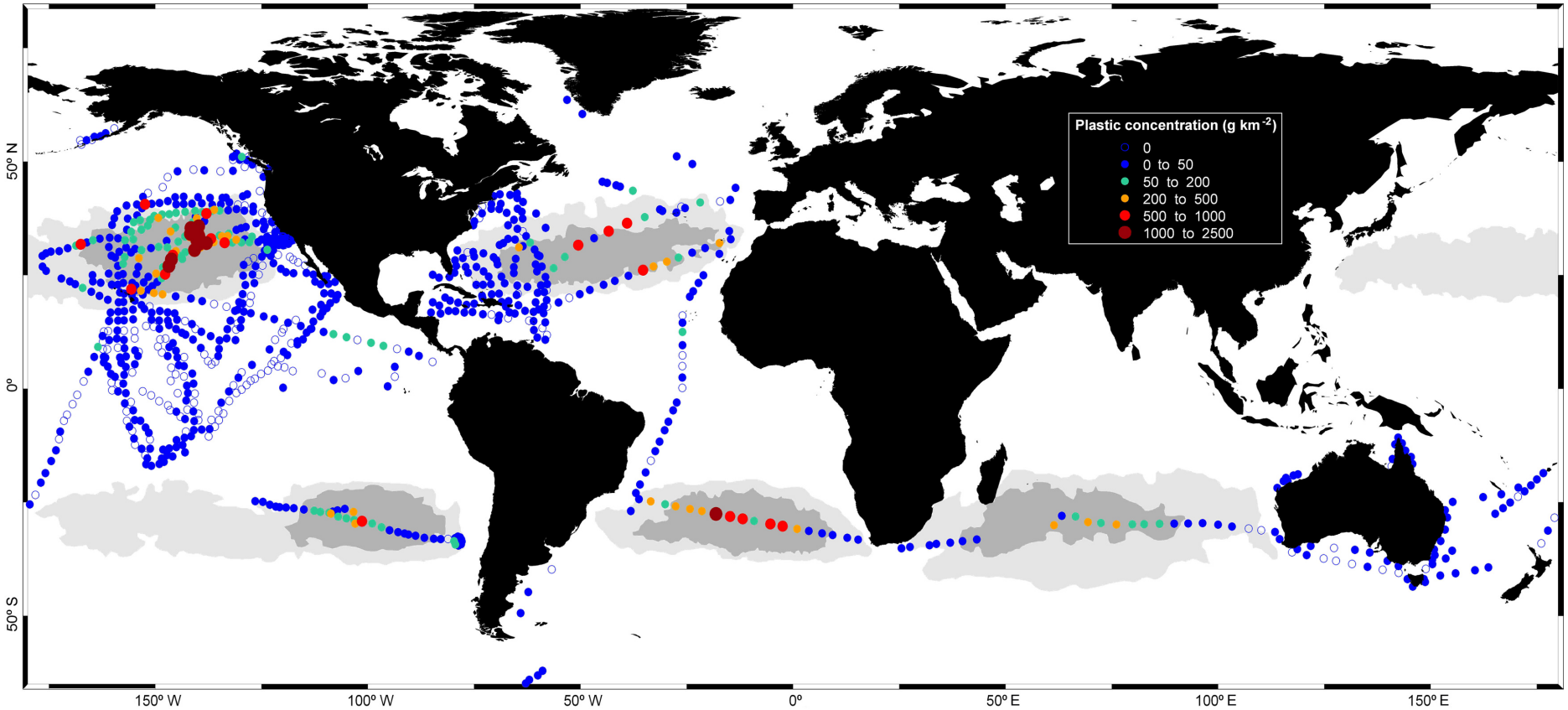

Fig. S2. Measurements of plastic concentrations without correction by wind conditions (non-corrected dataset). Color circles indicate mass concentrations (legend on top right). The dataset includes average concentrations in 851 sites (3070 surface net tows). Low estimate of plastic load was derived from this dataset.

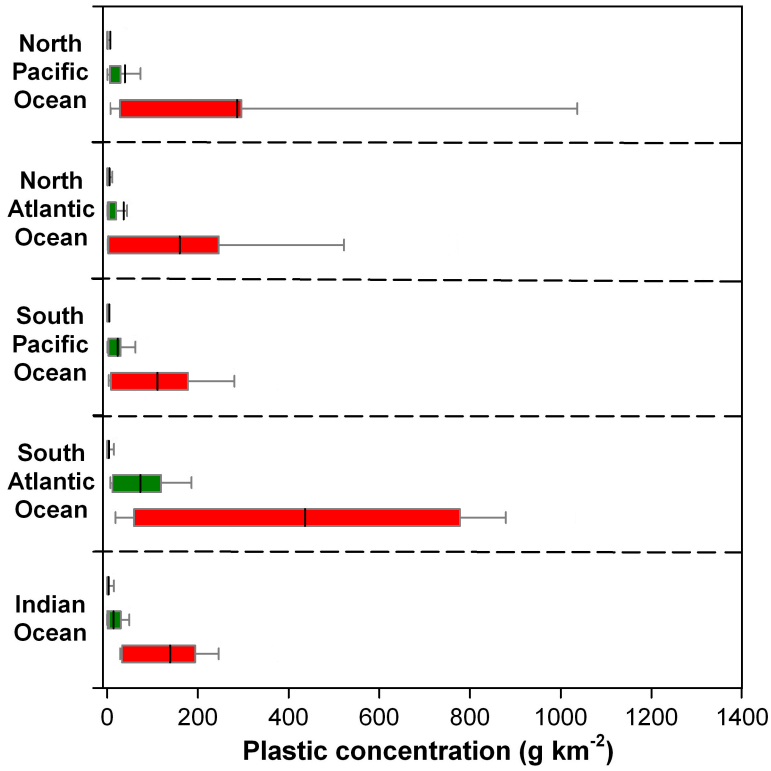

Fig. S3. Ranges of surface plastic concentrations calculated from the non-corrected database. Non-accumulation zone (blue boxes), outer accumulation zone (green boxes) and inner accumulation zone (red boxes). The boundaries of the boxes indicate the 25th and 75th percentiles, the black lines within the box mark the mean, and the whiskers above and below the boxes indicate the 90th and 10th percentiles. Data used for this graph are mapped in Fig. S2.

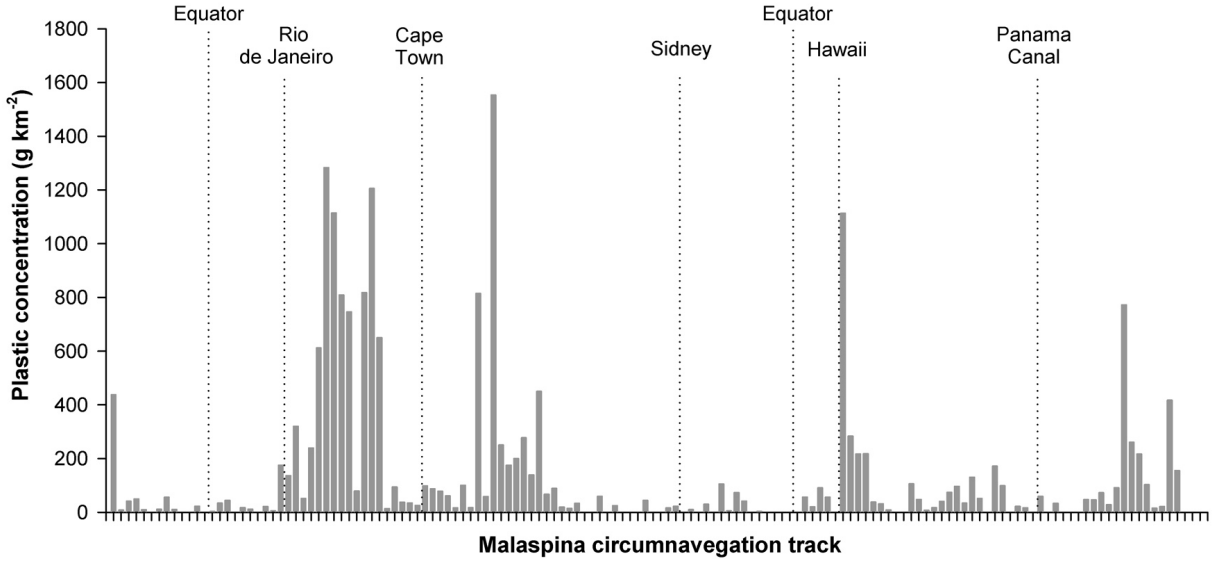

Fig. S4. Plastic concentrations along the Malaspina Circumnavigation from Cadiz to Cadiz (Spain). Every sampling site (blue circles in Fig. S1) is marked with a tick in the horizontal axis.

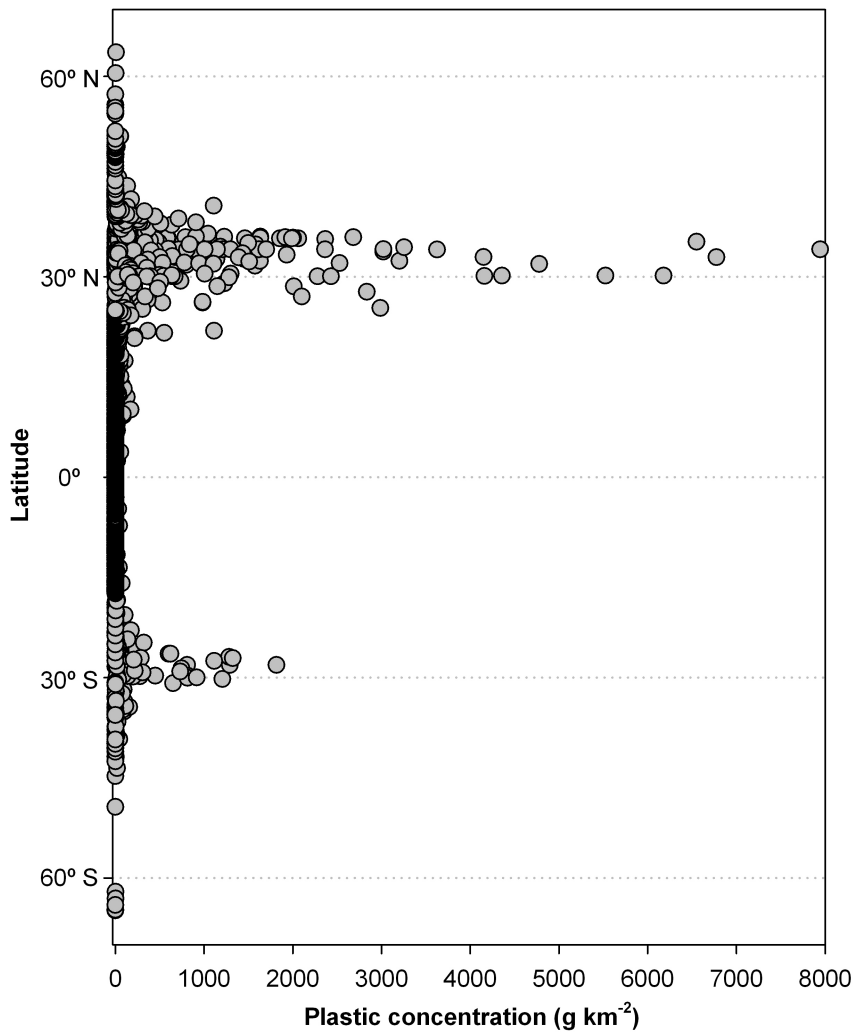

Fig. S5. Plastic concentrations as a function of latitude.

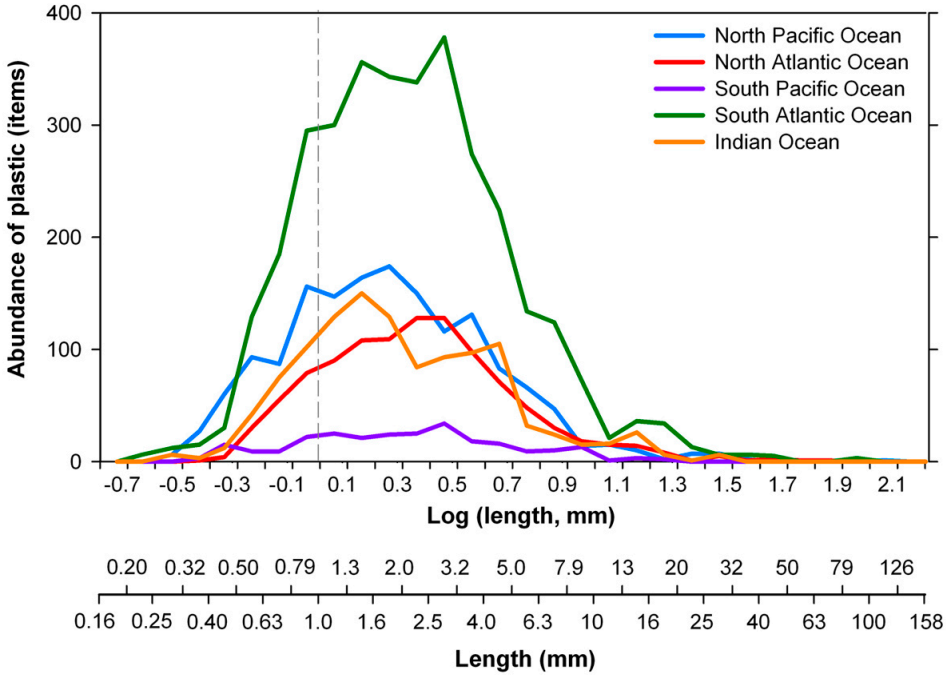

Fig. S6. Size distributions of plastic fragments by ocean basin. Size distributions were built with the plastic items collected along the circumnavigation: 1565 in North Pacific Ocean, 1043 items in North Atlantic Ocean, 259 items in South Pacific Ocean, 3339 items in South Atlantic Ocean, and 1153 items in Indian Ocean. The gap in the plastic size distributions below 1 mm was present in all ocean basins. Dashed vertical line corresponds to 1 mm size limits.

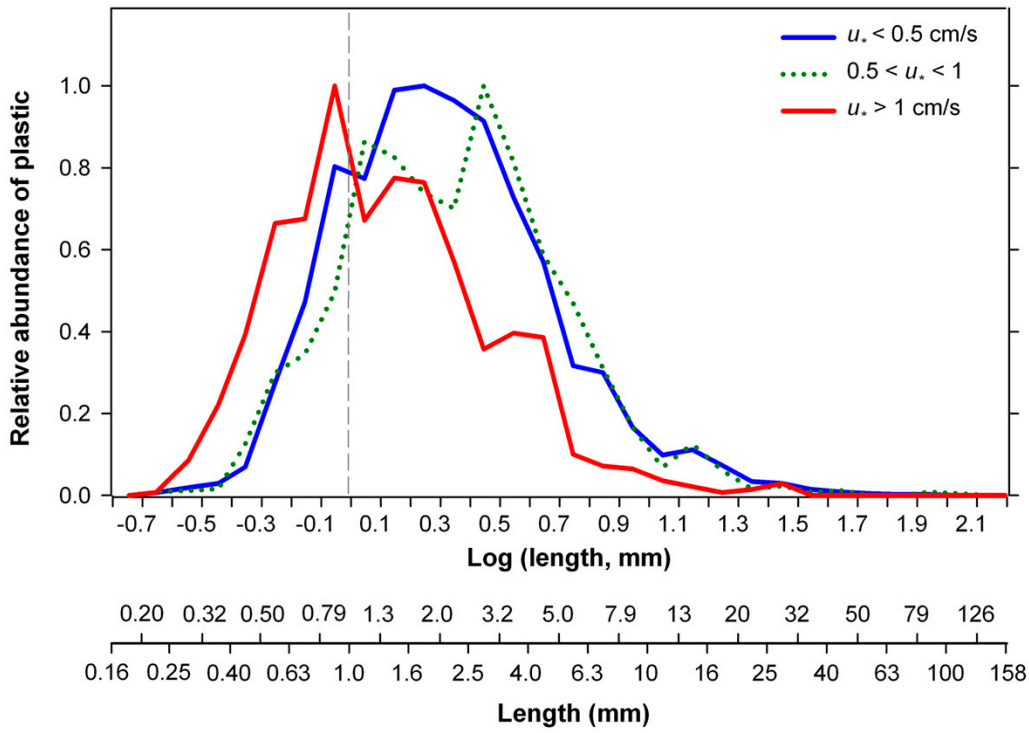

Fig. S7. Size distributions of surface plastic fragments for different wind conditions. Wind categories were established according to the u_* thresholds at which the effect of wind mixing on surface plastic abundance are predicted to be low (< 0.5 cm/s; 4184 plastic items), moderate (0.5 – 1 cm/s, 2138 items) and high (> 1 cm/s, 1037 items) (S7). For comparative purposes, these size distributions are shown as abundance in relation to the maximal abundance in the size classes. The comparison of confidence intervals of the means by inferential statistic only showed significant differences between the size distribution at high wind stress (> 1 cm/s) and the other two size distributions (< 0.5 cm/s and 0.5 – 1 cm/s). We found higher relative abundance of small particles (< 1 mm) in tows with high wind stress. The surface abundance of particles must decrease with wind stress due to vertical turbulent diffusion of buoyant particles throughout the surface wind-mixed layer. However, turbulence also leads to a size-selective increase of the vertical velocity resulting from the positive buoyancy of the particles (S8, S9). Theoretical considerations and empirical results evidence that upward velocities of particles sized around the Kolmogorov micro-scale (λ, the smallest length scale of the turbulence eddies) are very sensitive to turbulence levels. Their upward velocity may increase by two orders of magnitude more than those larger or smaller than λ (S9). Given that λ ranges from 0.3 to 2 mm for the wind-driven oceanic turbulence (S10), this process could explain the preferential accumulation of particles in the lower part of our size spectrum at high wind stress since they are around the same size as λ. These results allow us to conclude that the gap below 1 mm is not related to the wind effect.

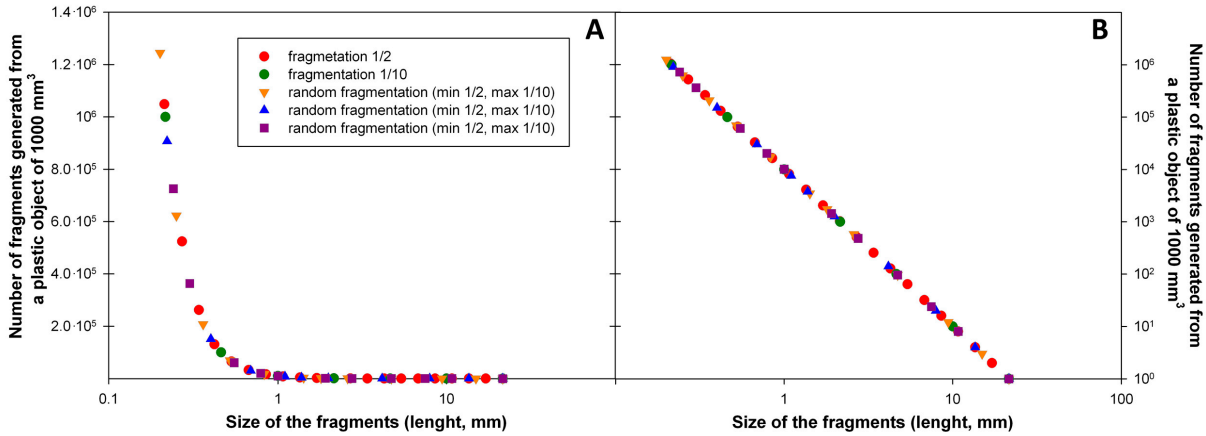

Fig. S8. Number of fragments generated from a plastic object of 1000 mm^3 using different fragmentation modes (see legend in A). Y-axis is lineal in A, and logarithmic in B. The length of the pieces was computed as $(volume/\alpha)^{1/3}$, being $\alpha = 0.1$. A plastic object successively broken down into half (fragmentation 1/2) would generate 2^n pieces, with n being the number of times broken down. And a plastic object successively broken down into ten pieces (fragmentation 1/10) would generate 10^n pieces. Note that the number of fragments of a specific size that a plastic object may generate depends on the original volume of the object, but it is independent of the number of pieces generated in each fragmentation event (e.g. 1/2 or 1/10) or the number of fragmentation events required (n). The exponent of the power law relationship described by the simulations is 3, regardless of the α value (shape of the object) used in the simulation. Therefore, a stable input and fragmentation of large plastic objects should lead to a power-law size distribution with a scaling exponent of 3. The exponent of the power-law part in the observed size distribution (size range: 5-100 mm, 14 size classes) confirmed this prediction (2.93 ±0.08 at calm conditions, Fig. 3; 2.98 ±0.13 using all tows in the circumnavigation, Fig. S10). This finding suggests that the fragmentation progressively proceeds in the three spatial dimensions of the objects (length, width and height), as observed in experiments of accelerated aging of plastic material (S11). Accordingly, the abundance-size distribution derived from fragmentation would depend on the large-plastic volume entering the ocean, being independent of plastic shape.

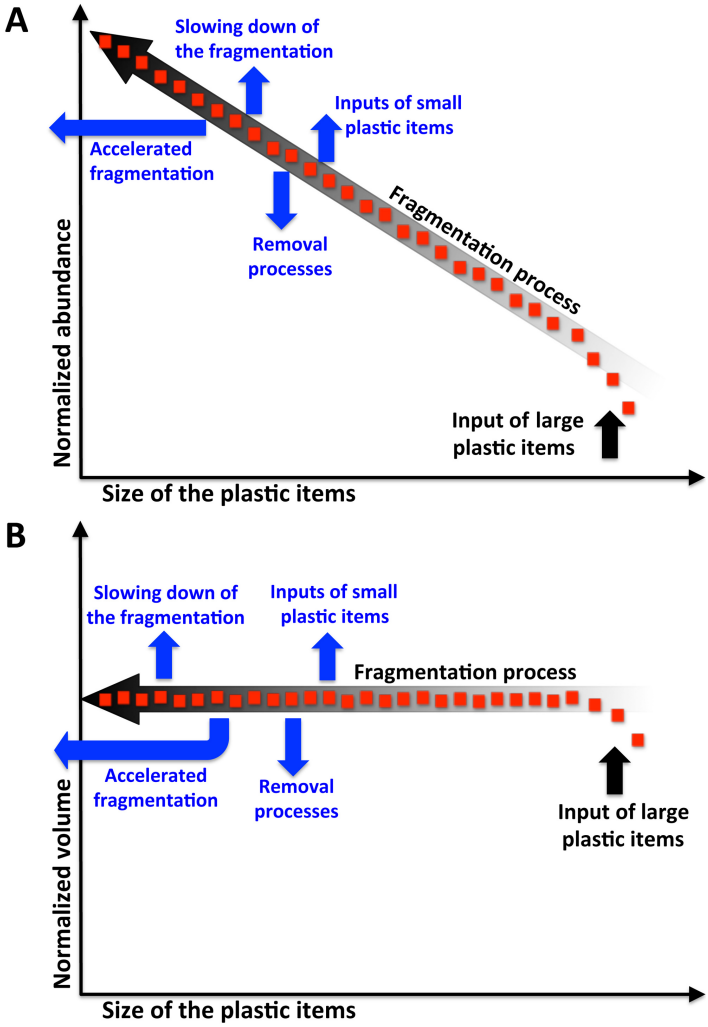

Fig. S9. Conceptual diagram of the main processes determining the shape of the size distribution of plastic in surface waters, in normalized abundance (A) and normalized volume (B). The power dependence of abundance on size can be linearized on a double log plot (red dots in A). Likewise, the log-log distribution of normalized volume by size classes should remain steady (red dots in B). Several processes (in blue) may lead to deviations from the log-log linearity. Domes or upward shifts in the linear size distribution can be caused by slowing down of the fragmentation process or significant inputs of small plastic items (e.g. industrial resin pellets). Troughs and gaps in the size distribution can be related to the acceleration of the fragmentation process or the occurrence of significant removal of plastic fragments (e.g. ingestion). Our study focus on an important trough in the plastic size spectrum (from few mm to microns), but cases of higher abundances toward small particles can be found in coastal marine environments (waters (S12) and sediments (S13, S14)) and lakes (S15). These small particles may be derived from fragmentation at sea but also from terrestrial inputs (e.g. textile fibers, microbeads used in cosmetic products), as suggested by some of these authors (S15). Indeed, textile fibers and microbeads are common in near shore environments, while they were negligible in our open-ocean sampling. Fragments, or broken pieces of larger objects, composed the majority of plastic items collected in the Malaspina Circumnavigation, in agreement with other samplings crossing plastic accumulation zones in the open ocean (S1, S16).

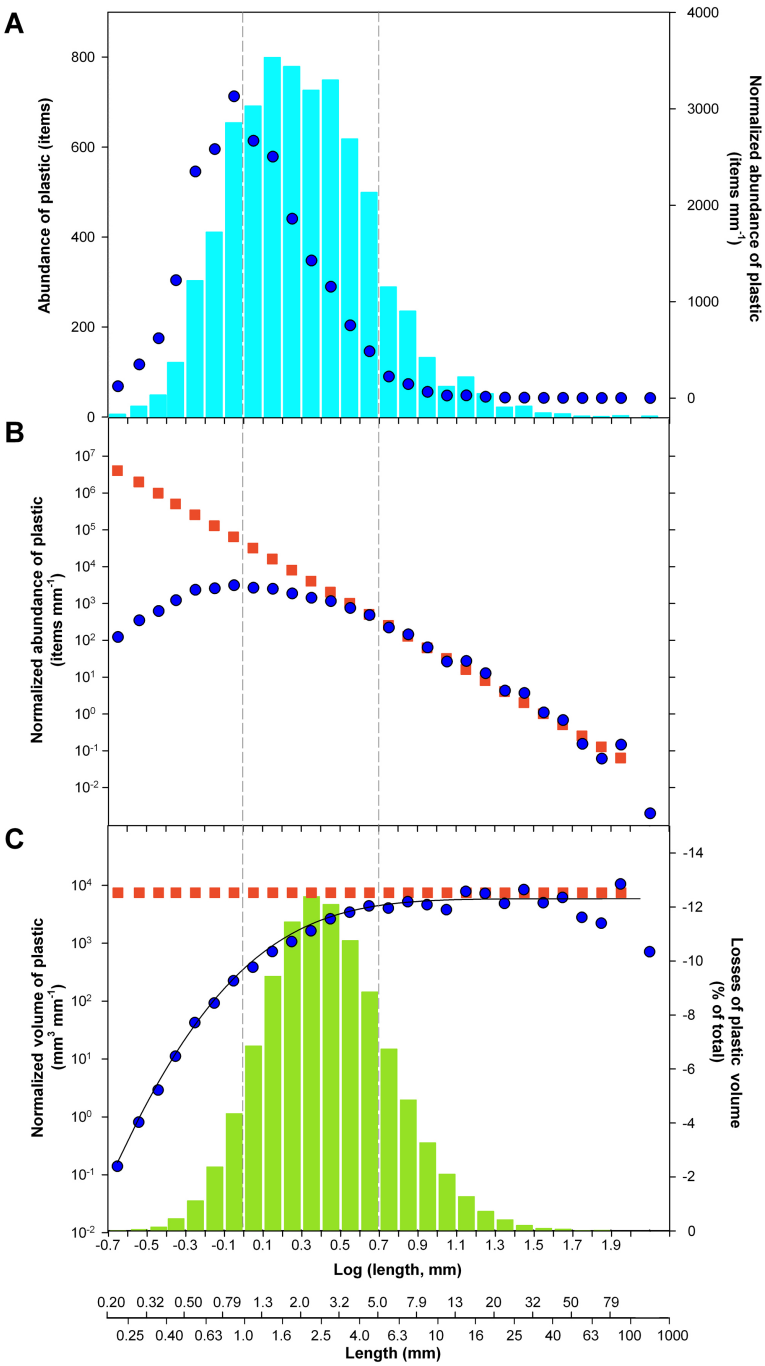

Fig. S10. Size distribution of plastic debris built with the material collected in all surface net tows in the Malaspina Circumnavigation (7359 items). (*A*) Size distribution in abundance (light blue bars) and normalized abundance (blue circles). (*B*) Measured (blue circles) and modeled (red squares) size distributions of normalized abundance of plastic in logarithmic scale. (*C*) Measured (blue circles) and modeled (red squares) size distributions of plastic in normalized volume. Green bars indicate the estimated losses of plastic volume by size class (Δ_i). Black line shows the measured size distribution after smoothing with a Weibull function (black line, R = 0.9921, $p < 0.0001$).

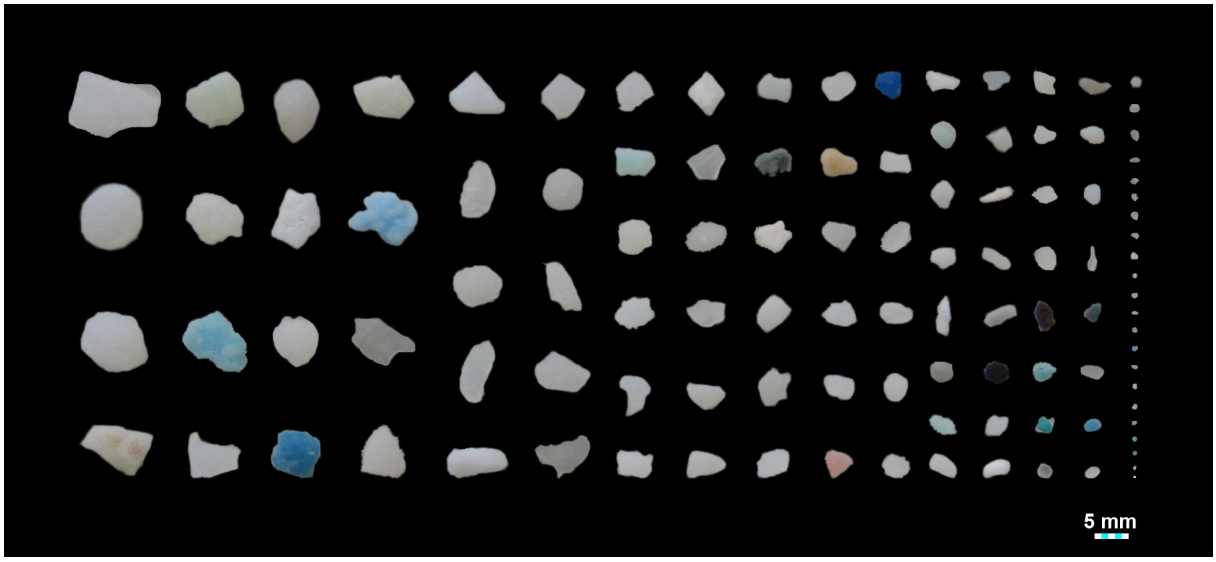

Fig. S11. Plastic fragments sampled on the ocean surface. This photography corresponds to the plastic items collected in a net tow in the South Atlantic Gyre.

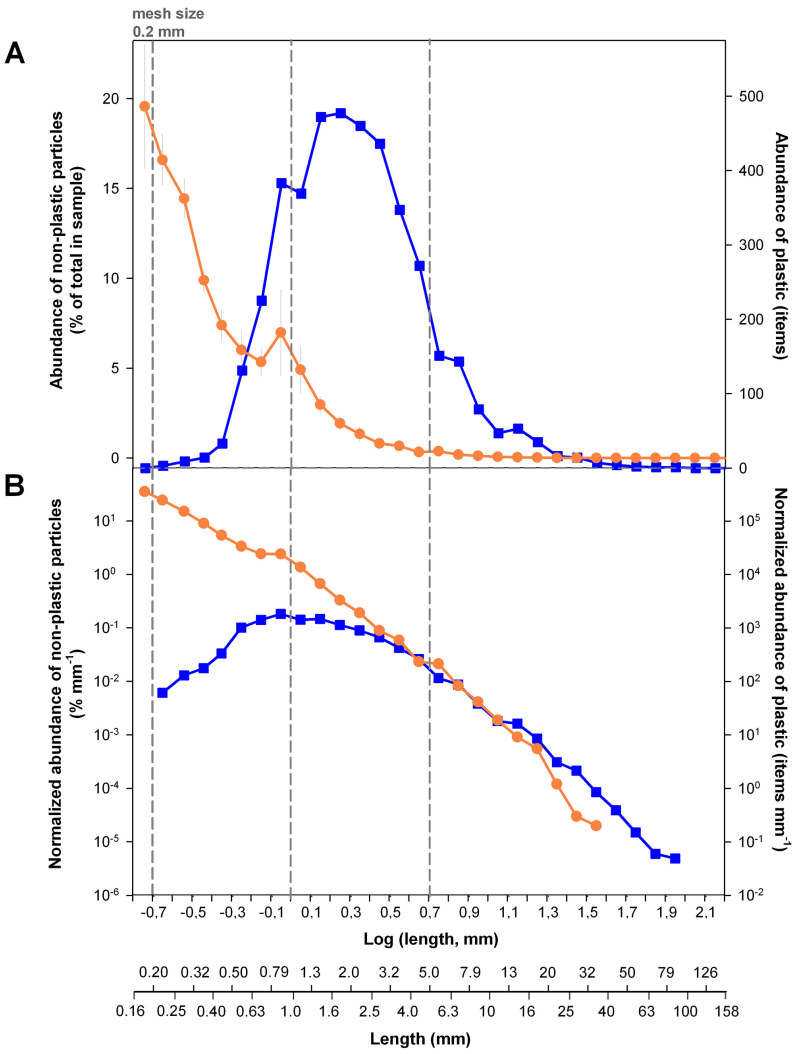

Fig. S12. Size distribution of non-plastic particles at six sites evenly distributed along the Malaspina circumnavigation (see Fig. S1 for location). (A) Size distribution in abundance. Orange line shows the averaged size distribution of non-plastic particles, computed as percentage of total in each sample to avoid over-representing the weight of samples with higher plankton abundance (left axis). Blue line shows the size distribution of plastic particles (right axis). (B) Size distribution in abundance normalized by the width (in mm) of the size class. Non-plastic particles are shown with orange line and plastic debris with blue line. The size distribution of non-plastic particles followed the expected power shape, with increasing abundances towards smaller sizes. The surface net used a 0.2-mm mesh, although it also collected abundant non-plastic particles in the 0.16-0.20 mm class likely due to mesh clogging. Vertical dashed lines show the thresholds of 0.2, 1.0 and 5.0 mm.

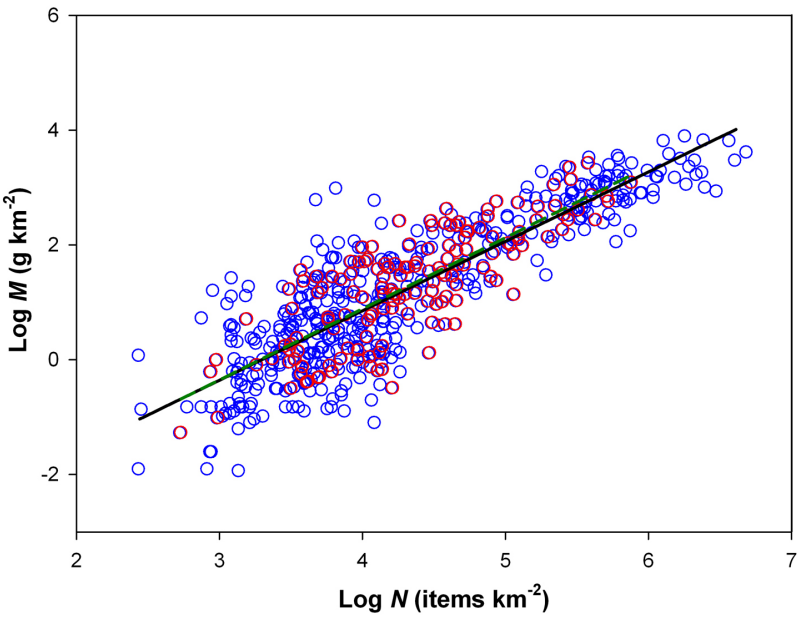

Fig. S13. Relationship between mass (*M*) and numerical (*N*) concentrations of plastic debris measured in the present study (*n* = 166, red open circles) and data from the literature (*n* = 404, blue open circles; refs. S2, S3, S17). Black line shows the log-log linear-square fitting on the whole dataset (log *M* (g km^{-2}) = 1.21· log *N* (items km^{-2}) - 3.99; *n* = 570, *r* = 0.8538, *p* < 0.0001). Green dashed line shows the log-log linear-square fitting on own data. Results suggest that the average size of plastic debris measured in Malaspina Circumnavigation is similar to that found for other world regions.

Supplementary References

S1. Law KL, et al. (2010) Plastic Accumulation in the North Atlantic Subtropical Gyre. *Science* 329:1185-1188.

S2. Doyle MJ, Watson W, Bowlin NM, Sheavly SB (2011) Plastic particles in coastal pelagic ecosystems of the Northeast Pacific ocean. *Mar Environ Res* 71:41-52.

S3. Goldstein MC, Rosenberg M, Cheng L (2012) Increased oceanic microplastic debris enhances oviposition in an endemic pelagic insect. *Biol Lett* doi: 10.1098/rsbl.2012.0298.

S4. Eriksen M, et al. (2013) Plastic pollution in South Pacific Subtropical Gyre. *Mar Pollut Bull* 15: 71-76.

S5. Reisser J, et al. (2013). Marine plastic pollution in waters around Australia: characteristics, concentrations, and pathways. *PLoS ONE* 8(11): e80466. doi:10.1371/journal.pone.0080466.

S6. Law KL, et al. (2014) Distribution of surface plastic debris in the eastern Pacific Ocean from an 11-year dataset. *Environ Sci Technol* 48:4732-4728.

S7. Kukulka T, Proskurowski G, Morét-Ferguson S, Meyer DW, Law KL (2012) The effect of wind mixing on the vertical distribution of buoyant plastic debris. *Geophys Res Lett* 39: L07601, doi: 10.1029/2012GL051116.

S8. Wang LP, Maxey MR (1993) Settling velocity and concentration distribution of heavy particles in homogeneous, isotropic turbulence. *J Fluid Mech* 256:27–68.

S9. Ruiz J, Macías D, Peters F (2004) Turbulence increases the average settling velocity of phytoplankton cells. *PNAS* 101: 17720–17724.

S10. Jiménez, J (1997) Oceanic turbulence at millimeter scales. *Sci Mar* 61(1): 47–56.

S11. Yakimets I, Lai D, Guigon M (2004) Effect of photooxidation cracks on behaviour of thick polypropylene samples. *Polym Degrad Stabil* 86:59–67.

S12. Cole M, et al. (2014) Isolation of microplastics in biota-rich seawater samples and organisms. Sci Rep 4:4528, doi: 10.1038/srep04528.

S13. Vianello A, et al. (2013) Microplastic particles in sediments of Lagoon of Venice, Italy: First observations on occurrence, spatial patterns and identification. *Estuar Coast Shelf Sci* 130:54-61.

S14. Browne, MA, Galloway TS, Thompson R.C. (2010). Spatial patterns of plastic debris along estuarine shorelines. *Environ Sci Technol* 44, 3404e3409.

S15. Eriksen M, et al. (2013a) Microplastic pollution in the surface waters of the Laurentian Great Lakes. *Mar Pollut Bull* 77:177-182.

S16. Morét-Ferguson S, et al. (2010) The size, mass, and composition of plastic debris in the western North Atlantic Ocean. *Mar Poll Bull* 60:1873-1878.

S17. Gilfillan LR, Ohman MD, Doyle MJ, Watson W (2009) Occurrence of plastic micro-debris in the southern California Current system. *Cal Coop Ocean Fish* 50:123–133.